

Effective structure of a system with continuous polydispersity

Palak Patel,^{1,2} Manoj Kumar Nandi,¹ Ujjwal Kumar Nandi,^{1,2} and Sarika Maitra Bhattacharyya^{1,2, a)}

¹⁾*Polymer Science and Engineering Division, CSIR-National Chemical Laboratory, Pune-411008, India*

²⁾*Academy of Scientific and Innovative Research (AcSIR), Ghaziabad 201002, India*

In a system of N particles, with continuous size polydispersity there exists $N(N-1)$ number of partial structure factors making it analytically less tractable. A common practice is to treat the system as an effective one component system which is known to exhibit an artificial softening of the structure. The aim of this study is to describe the system in terms of M pseudo species such that we can avoid this artificial softening but at the same time have a value of $M \ll N$. We use potential energy and pair excess entropy to estimate an optimum number of species, M_0 . We then define the maximum width of the polydispersity, $\Delta\sigma_0$ that can be treated as a monodisperse system. We show that M_0 depends on the degree and type of polydispersity and also on the nature of the interaction potential, whereas, $\Delta\sigma_0$ weakly depends on the type of the polydispersity, but shows a stronger dependence on the type of interaction potential. Systems with softer interaction potential have a higher tolerance with respect to polydispersity. Interestingly, M_0 is independent of system size, making this study more relevant for bigger systems. Our study reveals that even 1% polydispersity cannot be treated as an effective monodisperse system. Thus while studying the role of polydispersity by using the structure of an effective one component system care must be taken in decoupling the role of polydispersity from that of the artificial softening of the structure.

I. INTRODUCTION

Most systems that can be found in nature are inherently polydisperse. Polydispersity can be of different kinds like in size, in mass, and also in the shape of the particles. Also, the type of polydispersity and the degree of it varies with systems. Polydispersity brings variation in the properties of the material and there are specially designed controlled experiments to create monodisperse particles^{1,2}. However, in some cases polydispersity is a desirable property. The size polydispersity is one of the most common types and it has been found that systems beyond certain value of polydispersity, known as the terminal polydispersity are good glass former³⁻⁹. It was shown that in a polydisperse system due to an increase in surface free energy, the crystal nucleation is suppressed promoting glass formation¹⁰. Thus in study of supercooled liquids, polydisperse systems play an important role.

In recent time, it has been shown that structure plays an important role in the dynamics of glass forming supercooled liquids¹¹⁻¹⁹. Since polydisperse systems are good glass former describing the structure of these systems becomes important. For a continuous polydisperse system, the number of species is the number of particles in the system. In this case, describing the system's partial structure in terms of independent species becomes an impossible task. Thus it is common practice to treat a polydisperse system in terms of an effective one component system²⁰⁻²⁴. However, it has been shown that we not only lose a large deal of information of the system by pre averaging the structure, the properties of the

liquid thus predicted can also give spurious results.^{25,26}. Truskett and coworkers²⁵ have shown that for moderate polydispersity the thermodynamic quantities like the pair excess entropy obtained from the effective one component radial distribution function (rdf) predicts that with an increase in interaction the static correlation becomes weaker thus predicting structural anomaly. The study showed that when the system is expressed in terms of 60 pseudo neighbors and the excess entropy is calculated in terms of the partial structure factors (radial distribution functions), this structural anomaly disappears. Weysser *et. al.* while working with Mode coupling theory have shown that for a polydisperse system, we need to provide information about the partial structure factors to obtain the correct dynamics²⁶. Ozawa and Berthier have highlighted the fact that for a system with continuous size polydispersity the contribution from the mixing entropy term diverges²⁷. This makes the calculation of entropy and any other dependent quantity ill-defined. They showed by calculating the inherent structure properties that when the position of the particles with similar sizes is exchanged, the system stays in a similar basin. This modifies the vibrational entropy, which also has the same mixing entropy term. The process allowed them to group particles into a certain finite number of pseudo species leading to a finite value of the mixing entropy. These studies thus emphasize the importance of describing the structure of a polydisperse system in terms of the partial structure factors of the pseudo species.

The present study attempts to develop a general framework to describe the structure of a system having continuous polydispersity. As discussed before, for a system with continuous polydispersity the number of species is the same as the number of particles which makes it difficult to describe the structure. We also know that describing all the particles in terms of a single species does

^{a)}Electronic mail: mb.sarika@ncl.res.in

not work. So the aim of this study is to describe the system in terms of M pseudo species such that the properties of this system are the same as the original system. The questions that we ask are i) Can we determine the minimum number of pseudo species ' M'_0 ' required to describe the structure of the system? ii) Is this dependent on the property that we study? iii) Does it depend on the degree and nature of polydispersity? iv) Does it depend on the interaction potential?

To answer these questions we use the route of calculating thermodynamic quantities which can be obtained from the structure of the liquid. Namely the potential energy of the system and the pair excess entropy. Note that the former is a linear function of the structure whereas the latter is a nonlinear function of the structure and thus can have different sensitivities to the effective structure. We find that by studying these above mentioned thermodynamical quantities, we can determine a value of M_0 . It depends on the type of polydispersity, the degree of polydispersity, and the interaction potential. We also provide an estimate of the width of polydispersity that can be treated like a one component system. This width appears to depend primarily on the interaction potential of the system. Systems with longer range and softer interaction potential have a better tolerance towards polydispersity. In these cases, systems with a wider spread of size can be addressed in terms of a one component system.

The organization of the rest of the paper is the following. Section II contains the simulation details. In Section III, we discuss the methods used for evaluating the various quantities of interest. Section IV contains results with discussions and the paper ends with a brief conclusion in Section V.

II. SIMULATION DETAILS

In this study, we perform molecular dynamics simulations for three-dimensional polydisperse system with continuous size polydispersity in the canonical ensemble. The system contains $N=1000-4000$ particles in a cubic box of volume V . The number density for all the systems is $\rho = N/V = 1.0$. In our simulations, we have used periodic boundary conditions and Nosé-Hoover thermostat with integration timestep 0.001τ . The time constants for the Nosé-Hoover thermostat are taken to be 100 timesteps. We have carried out the molecular dynamics simulations using the LAMMPS package²⁸. The study involves two different kinds of systems with respect to size polydispersity, constant volume fraction (CVF) and Gaussian (as shown in Fig. 1) and three different kinds of interaction potentials. The distributions of the particle size are continuous. This means each of the N particles has a different radius. The form of the constant volume fraction distribution is given by⁸,

$$P_1(\sigma) = \frac{A}{\sigma^3}, \quad \sigma \in [\sigma_{max}, \sigma_{min}] \quad (1)$$

TABLE I: Details of the size distributions, constant volume fraction and Gaussian, for different degrees of polydispersity $PDI = \frac{\sqrt{\langle \sigma^2 \rangle - \langle \sigma \rangle^2}}{\langle \sigma \rangle}$. The maximum, σ_{max} , and minimum σ_{min} , values of the diameter of the particles. The volume fraction η is also given showing an increase in η with degree of polydispersity.

Distribution	PDI %	σ_{max}	σ_{min}	$\Delta\sigma$	η
$P_1(\sigma)$	5%	1.1	0.92	0.18	0.53
	10%	1.21	0.85	0.36	0.54
	15%	1.34	0.8	0.54	0.56
$P_2(\sigma)$	5%	1.15	0.85	0.3	0.53
	10%	1.3	0.7	0.6	0.54
	15%	1.45	0.55	0.9	0.56

where A is the normalization constant and σ_{max} and σ_{min} are the maximum and minimum values of particle diameter. σ_{max} and σ_{min} values are given in Table.I. The degree of polydispersity is quantified by⁸ the normalized root mean square deviation

$$PDI = \frac{\sqrt{\langle \sigma^2 \rangle - \langle \sigma \rangle^2}}{\langle \sigma \rangle}$$

Where $\langle \dots \rangle$ defines the average of the particle size distribution.

The Gaussian distribution is given by

$$P_2(\sigma) = \frac{1}{\sqrt{2\pi}\delta^2} \exp \frac{-(\sigma - \langle \sigma \rangle)^2}{2\delta^2} \quad (2)$$

Where δ is the standard deviation. In this distribution we consider $\sigma_{max/min} = \langle \sigma \rangle \pm 3\delta$. The degree of polydispersity is quantified by,

$$PDI = \frac{\sqrt{\langle \sigma^2 \rangle - \langle \sigma \rangle^2}}{\langle \sigma \rangle} = \frac{\delta}{\langle \sigma \rangle}$$

For all the polydisperse systems the particle sizes are such chosen that $\langle \sigma \rangle = \int P(\sigma)\sigma d\sigma = 1$ and is kept as the unit of length for all the systems studied here.

The three different interaction potentials studied here are inverse power law (IPL) potential, Lennard-Jones (LJ) potential and its repulsive counterpart the Weeks-Chandler-Andersen (WCA) potential. The inverse power law potential (IPL) between two particles i and j is given by,^{8,29}

$$U(r_{ij}) = \begin{cases} \epsilon_{ij} \left(\frac{\sigma_{ij}}{r_{ij}}\right)^{12} + \sum_{l=0}^2 c_{2l} \left(\frac{r_{ij}}{\sigma_{ij}}\right)^{2l}, & \left(\frac{r_{ij}}{\sigma_{ij}}\right) \leq x_c \\ 0, & \left(\frac{r_{ij}}{\sigma_{ij}}\right) > x_c \end{cases} \quad (3)$$

The constants c_0, c_2 and c_4 are selected such that the potential becomes continuous up to its second derivative at the cutoff $x_c = 1.25\sigma_{ij}$.

The LJ potential between the two particles i and j is described using truncated and shifted LJ potential³⁰;

$$U(r_{ij}) = \begin{cases} U^{(LJ)}(r_{ij}; \sigma_{ij}, \epsilon_{ij}) - U^{(LJ)}(r_{ij}^{(c)}; \sigma_{ij}, \epsilon_{ij}), & r_{ij} \leq r_{ij}^{(c)} \\ 0, & r_{ij} > r_{ij}^{(c)} \end{cases} \quad (4)$$

where $U^{(LJ)}(r_{ij}; \sigma_{ij}, \epsilon_{ij}) = 4\epsilon_{ij}[(\frac{\sigma_{ij}}{r_{ij}})^{12} - (\frac{\sigma_{ij}}{r_{ij}})^6]$. The cutoff for the LJ system is $r_{ij}^{(c)} = 2.5\sigma_{ij}$ and for the WCA system is $r_{ij}^{(c)} = 2^{1/6}\sigma_{ij}$.³¹ The interaction strength between two particles i and j is $\epsilon_{ij} = 1.0$. $\sigma_{ij} = \frac{(\sigma_i + \sigma_j)}{2}$, where σ_i is a diameter of particle i and it varies according to the system. Length, temperature and times are given in units of $\langle \sigma \rangle$, ϵ_{ij} and $(\frac{m\langle \sigma \rangle^2}{\epsilon_{ij}})^{1/2}$ respectively. For all state points, the equilibration is performed for $100\tau_\alpha$ (τ_α is the α -relaxation time) and three to five independent samples are analyzed. As discussed later, in this work both potential energy and pair excess entropy are calculated using the partial structure factors. In a system with continuous polydispersity, each particle has a different diameter. So there are $\frac{N \times N}{2}$ partial radial distribution functions. For $N = 1000$ there are thus 500,000 partial rdf and with increase in N this number grows as N^2 . Calculating these many partial rdf with good precision is an impossible task. However, in this study, we divide the total system into M species. Particles with diameter range $(\sigma_{max} - \sigma_{min})/M$ are treated as a single species. Note that this is an approximation because the particle sizes in a single species are still different. With an increase in M this diameter range becomes narrow and the approximation leads to less error. The maximum value of M that we have used in this work is 26. Thus we have calculated at the most 338 partial rdf. Although the study is performed in the high temperature regime where the production run length is usually around $100\tau_\alpha$ where τ_α varies between 5 – 100, for this study to get a good precision of the partial rdf we require longer production run lengths to compensate for the poor particle averaging. For 5% PDI the production run length is 10^7 and for 15% PDI and 10% PDI the production run lengths are 10^7 for $T = 5.0-0.38$ and 6×10^7 for $T=0.36-0.2$

III. DEFINITION AND BACKGROUND

A. Radial distribution function

The partial radial distribution $g_{\alpha\beta}(r)$ is define as:

$$g_{\alpha\beta}(r) = \frac{V}{N_\alpha N_\beta} \left\langle \sum_{i=1}^{N_\alpha} \sum_{j=1, j \neq i}^{N_\beta} \delta(r - r_i + r_j) \right\rangle \quad (5)$$

Where V is the volume of the system, N_α , N_β are the number of α and β type of particles, respectively.

The effective one component radial distribution function, $g(r)$ can be written in terms of partial rdf of M species as.³²

$$g(r) = \sum_{\alpha, \beta=1}^M \chi_\alpha \chi_\beta g_{\alpha\beta}(r) \quad (6)$$

Where χ_α and χ_β are the mole fraction of α and β particles, respectively.

B. Potential energy

The per particle potential energy of the system can be exactly calculated from simulation E_{sim} . The same can also be

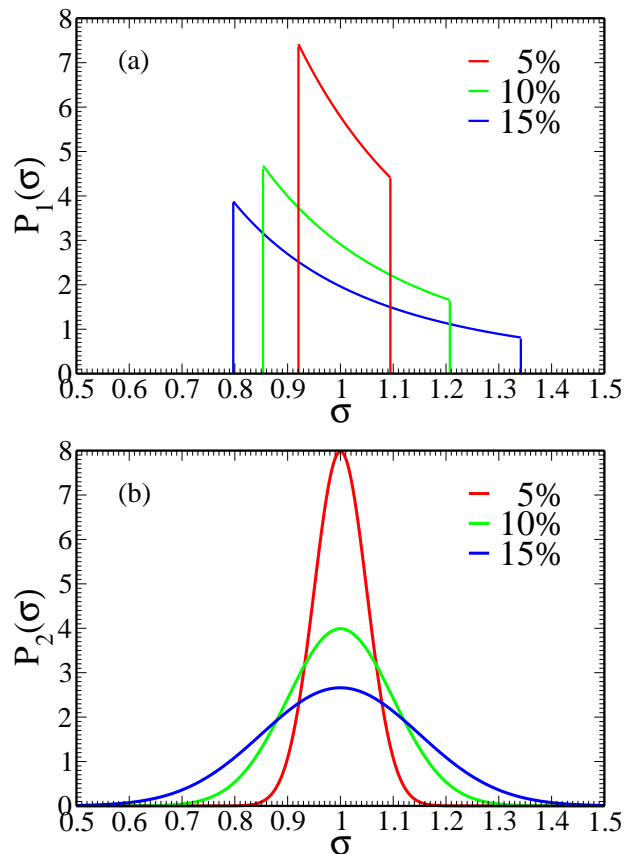


FIG. 1: Different kind of distributions (a) Constant volume fraction distribution, $P_1(\sigma)$ (b) Gaussian distribution, $P_2(\sigma)$. For the same degree of polydispersity, compared to $P_1(\sigma)$ the distribution is wider for $P_2(\sigma)$.

written in terms of the partial radial distribution function, E_2 .

$$E_2 = \frac{\rho}{2} \sum_{\alpha, \beta=1}^M \chi_\alpha \chi_\beta \int_0^\infty 4\pi r^2 U_{\alpha\beta}(r) g_{\alpha\beta}(r) dr \quad (7)$$

In the effective one component treatment the energy can be written as E_2^{eff} ,

$$E_2^{eff} = \frac{\rho}{2} \int_0^\infty 4\pi r^2 U(r) g(r) dr \quad (8)$$

C. Excess entropy

Excess entropy S_{ex} is a loss of entropy due to the interaction between the particle or in other words excess entropy is a difference between S_{total} and S_{ideal} at same temperature T and density ρ . The value of S_{ex} is always a negative. S_{ex} can be evaluated by thermodynamic integration (temperature density landscape)³³. Entropy at high temperature and low density is that of an ideal gas entropy. This S_{ideal} is a relative reference for any other state points entropy calculation. Other state point entropy can be calculated

using a combination of isotherms (Eq.9) and isochoric (Eq.10) paths, making sure that no phase transitions occurs along the selected path³³.

$$S_{ex}(T, V') - S_{ex}(T, V) = \frac{U(T, V') - U(T, V)}{T} + \int_V^{V'} \frac{P(V)}{T} dV \quad (9)$$

$$S_{ex}(T', V') - S_{ex}(T, V') = \int_T^{T'} \frac{1}{T} \left(\frac{\delta U}{\delta T} \right)_{V'} dT \quad (10)$$

Addition of Eq. 9 and Eq. 10 give the total excess entropy.

D. Pair Entropy

Using Kirkwood factorization³⁴, the excess entropy can also be expressed in terms of an infinite series,

$$S_{ex} = S_2 + S_3 + S_4 \dots \quad (11)$$

Where S_n is an entropy contribution due to n particle spatial correlation. The pair excess entropy, S_2 includes 80% of the total excess entropy³⁵. We can calculate S_2 from the partial rdf of M species³³-

$$\frac{S_2}{k_B} = -2\pi\rho \sum_{\alpha, \beta=1}^M \chi_\alpha \chi_\beta \int_0^\infty r^2 dr \{g_{\alpha\beta}(r) \ln g_{\alpha\beta}(r) - (g_{\alpha\beta}(r) - 1)\} \quad (12)$$

Where k_B is a Boltzmann constant.

If we do not consider the different species then the entropy for an effective one component system can be written as S_2^{eff} ,

$$\frac{S_2^{eff}}{k_B} = -2\pi\rho \int_0^\infty r^2 dr \{g(r) \ln g(r) - (g(r) - 1)\} \quad (13)$$

E. Onset temperature calculation from Inherent structure energy

While cooling a glass forming liquid from high temperatures at the onset temperature, T_{onset} the system's thermodynamic and dynamic properties deviate from its high-temperature behavior. There are different dynamical and thermodynamical measures of T_{onset} . The temperature predicted by each method is not identical but lies in a similar range. A comparison of the different methods is given in Ref.15. In this work, we will discuss the one calculated from the inherent structure energy and the other from the excess entropy.

The inherent structure energy is the potential energy evaluated at the local minimum of the energy reached from the configuration via the steepest descent procedure. As suggested earlier³⁶ the onset temperature is connected to the inherent structure energy. At high temperatures as the system is not influenced by the landscape properties, the average inherent structure energy is almost temperature independent. However below a certain temperature, where the landscape properties influence the system, the inherent structure energy starts to

decrease rapidly. Usually, the two different regimes are fitted to two straight lines and the point where these lines cross is identified as the onset temperature, T_{onset} .

F. Dynamics

In this work to characterize the dynamics we consider the self part of the overlap function $Q(t)$ defined as,³⁷

$$Q(t) = \frac{1}{N} \sum_{i=1}^N \langle \omega(|\mathbf{r}_i(t) - \mathbf{r}_i(0)|) \rangle \quad (14)$$

where the function $\omega(x)$ is 1 if $0 \leq x \leq a$ and $\omega(x) = 0$ otherwise. The parameter a is chosen to be 0.3, a value that is slightly larger than the size of the cage.

Note that the dynamics can also be obtained from self-intermediate scattering function $F_s(q, t)$ where $q = 2\pi/r_{max}$, r_{max} being the position of the first peak of the radial distribution function. Since relaxation times from $Q(t)$ and $F_s(q, t)$ behave very similarly at low temperature, we use $Q(t)$ for the dynamics.

IV. RESULT

A. Effective one-component description

As discussed before it is a common practice to describe the structure of a polydisperse system in terms of an effective one component system.

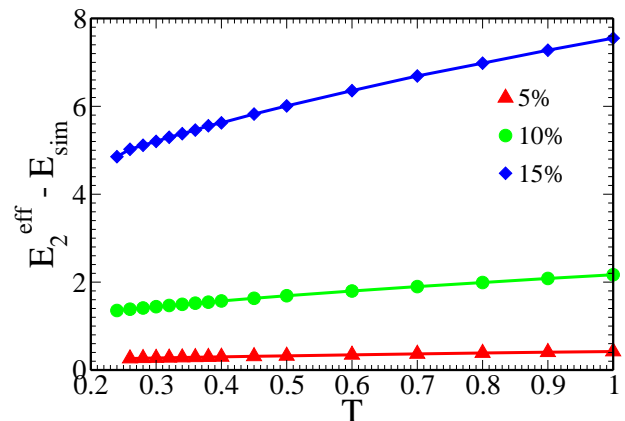


FIG. 2: The difference in energy obtained from effective one component radial distribution functions, E_2^{eff} and simulation, E_{sim} as a function of T at different PDIs. Here particles are interacting via IPL potential and the particle size distribution is given by $P_1(\sigma)$ (constant volume fraction distribution).

In Fig.2, we plot the difference between the average per particle potential energy of the species agnostic E_2^{eff} and that obtained from simulation E_{sim} for systems with different PDI values (5%,10% and 15%). In the simulation study, the particle sizes are obtained from $P_1(\sigma)$ distribution and they interact via IPL potential. In Fig.3 we also plot the S_{ex} and the

species agnostic S_2^{eff} for the above mentioned systems. Note that if the structure is described properly then $E_{sim} = E_2$ and S_2 is not exactly equal to S_{ex} but comprises of 80% of its value^{15,33,35,38-42}.

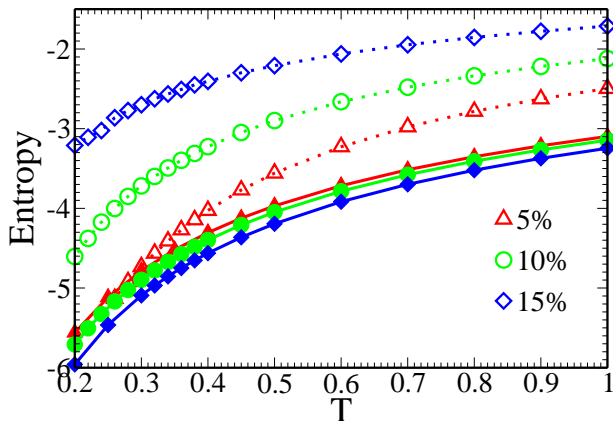


FIG. 3: Excess entropy, S_{ex} and effective one component pair excess entropy, S_2^{eff} (Eq.13) at different PDIs. Solid line with filled symbol represents S_{ex} and dotted line with open symbol represents S_2^{eff} . Here particles are interacting via IPL potential and the particle size distribution is given by $P_1(\sigma)$ (constant volume fraction distribution).

We find that as the PDI increases the difference between E_{sim} and E_2^{eff} and S_{ex} and S_2^{eff} increases. This clearly shows that as expected, with an increase in PDI the effective one component description of the system becomes less accurate. In Fig.4 we plot both the dynamics and the effective one component rdf of the systems. We find that within the temperature range studied here although the dynamics remains almost the same, with an increase in polydispersity the structure appears to soften. We have plotted the rdf at two temperatures, ($T=1.0$ and 0.5) and it appears that the softening is present in both temperatures. However, the fact that the difference between E_2^{eff} and E_{sim} reduces at low temperatures (Fig.2) do suggest that the softening also reduces with temperature. This artificial softening of the structure leads to the increase in E_2^{eff} and S_2^{eff} . Note that even for 5% polydispersity we find that the effective one component structure of the system fails to provide the correct value of the potential energy and the pair excess entropy. These results presented in Fig.2 and Fig.3 are not surprising but a confirmation of the observations made earlier^{25,26}.

B. Pseudo species and its dependence on degree of polydispersity

Describing the structure of a continuous polydisperse system can be challenging? Unlike in a discrete polydisperse system where each species has a finite number of particles and all of them have the same size, for a continuous polydisperse system the number of species is the same as the number of particles. However, let us assume that we describe a pseudo system where we divide the particles into M number of pseudo species (where $M < N$) in terms of the size of the particles. In

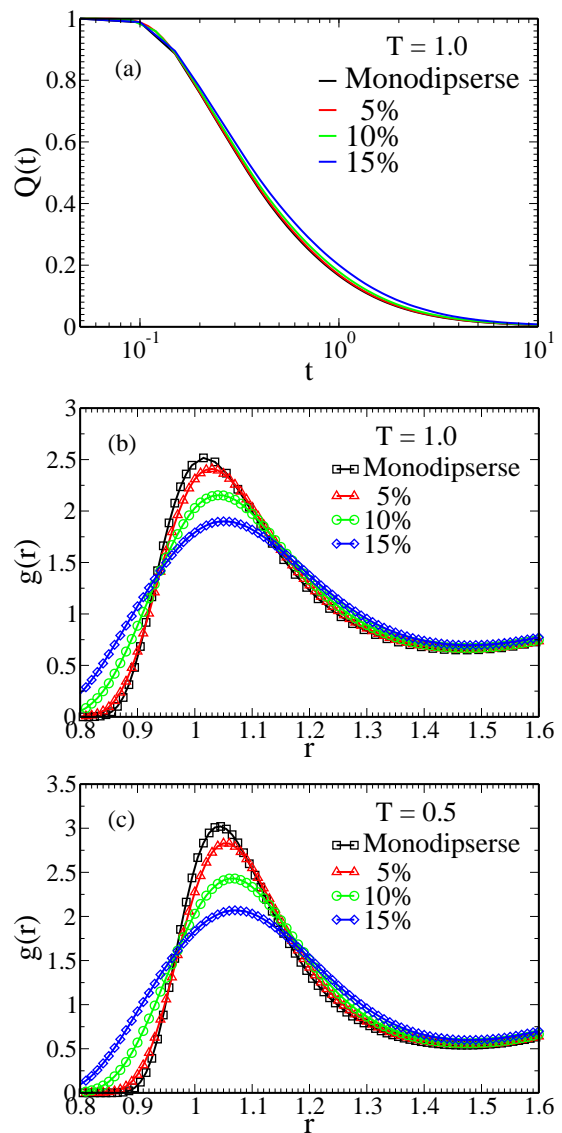


FIG. 4: (a) Dynamics of systems at different PDIs. The overlap function is plotted against time. (b) Effective one component radial distribution function of the systems at $T = 1.0$. (c) Same as Fig.4(b) at $T = 0.5$. Black square, red triangle, green circle and blue diamond represent a mono disperse system, 5% PDI, 10% PDI and 15% PDI, respectively. With an increase in PDI although the dynamics remains almost the same the structure shows a substantial softening. Here particles are interacting via IPL potential and the particle size distribution is given by $P_1(\sigma)$ (constant volume fraction distribution).

doing so we bunch particles with similar but different sizes, in a group and assign an average size to them. This introduces disparity in the actual size and the assigned size of the particles and leads to an error in describing the properties of the system. An extreme case of that ($M = 1$) can be seen in Fig.2 and Fig.3. For a fixed M , the maximum difference in the actual diameter of a particle and its assigned average

diameter is $\Delta\sigma/2M$. Thus with an increase in M this error reduces and at $M = N$ the pseudo system is exact. So the first question is can we describe the structure of a system in terms of an optimum number of species M_0 , where $M_0 \ll N$ such that the structure can provide a correct estimate of the thermodynamic quantities? If we can then how does M_0 depend on the degree of polydispersity?

In Fig.5(a) we plot $\frac{E_2}{E_{sim}}$ as a function of M , at two different temperatures for the different PDIs. For systems with a fixed value of PDI as we increase the value of M the E_2 decreases and after a certain value of M , $E_2 \simeq E_{sim}$. We find that this is weakly temperature dependent. For this work we consider that at $T = 1$ the minimum number of pseudo species for which $\frac{(E_2 - E_{sim})}{E_{sim}} < 0.01$ is M_0 . The value of M_0 is system dependent and as expected increases with the increase in PDI value as can be seen from Fig.5(b). Note that when determining M_0 this choice of the relative error (0.01) is arbitrary but practical. In principle, we can choose values much smaller or probably larger than this. However, later, while discussing the value of M_0 as obtained from entropy, we will see that this choice is reasonable.

Is the value of M_0 sensitive to the thermodynamic quantity that we calculate or is it universal? To answer this question we calculate the two body pair entropy for different values of M . We find that similar to the energy, as M increases the S_2 comes closer to S_{ex} (Fig.6). However, even for large values of M , S_2 is not equal to S_{ex} . This is because unlike the potential energy which can be exactly calculated in terms of the partial rdf, only a part of the excess entropy can be calculated from the rdf (Eq.11)^{15,33,35,38-42}. This makes it difficult to use the same methodology as used for potential energy to make an estimation of M_0 from entropy.

However, from our earlier studies, we know that if the structure of the liquid is described properly then the excess entropy and the two body pair entropy cross each other at a temperature, T_{cross} which can be considered as the onset temperature of the supercooled liquid dynamics¹⁵. This onset temperature can also be obtained from the change in the slope of the temperature dependence of the inherent structure energy³⁶ and also other methods¹⁵. As shown earlier the values of the onset temperatures obtained using these different methods are not exactly the same but they are in a similar range¹⁵.

In Fig.7 we plot the variation of T_{cross} with M for the different systems. For higher PDI, at small values of M , we cannot calculate T_{cross} which implies that S_2 is far away from S_{ex} and never crosses it as seen in Fig.6. However, from our other estimates of onset temperature, we know that we are in a temperature range where these two forms of entropy should cross. As M increases the two functions cross at some temperature T_{cross} . We find that initially T_{cross} increases with M and then after a certain value of M it shows a saturation. As mentioned before S_2 is not the total excess entropy of the system. There is no other method of calculating S_2 . Thus it is not possible to do a similar error estimation of pair excess entropy as done for the potential energy. However, the saturation of T_{cross} is an indication of the saturation of S_2 w.r. to M . We find that this saturation value of T_{cross} is in a similar range as the estimated onset temperature using the method of inherent structure energy (see Sec III E and Table II). In this plot we also mark the M_0 values as obtained from the potential energy. We find that the M value for which T_{cross} saturates falls in the similar range as M_0 . The val-

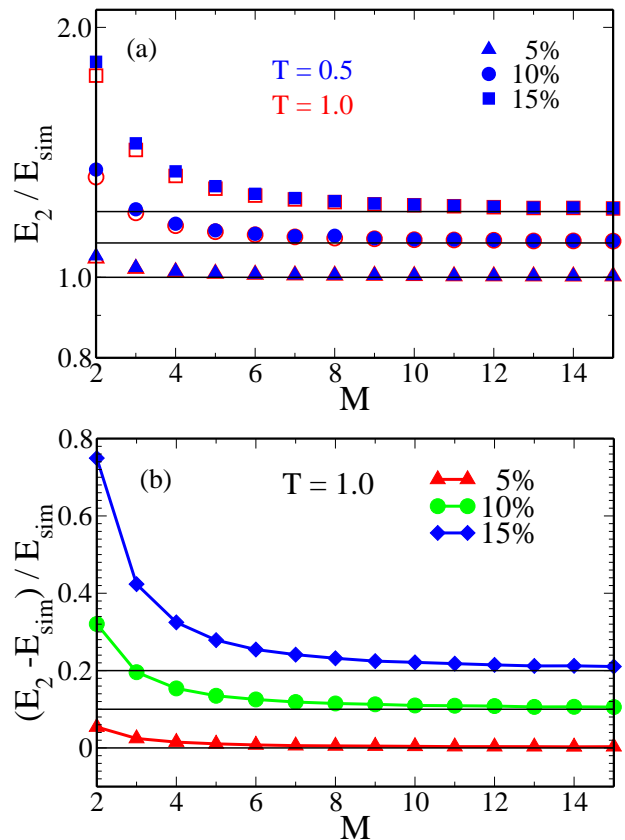


FIG. 5: Comparison between energy obtained from simulation, E_{sim} , and energy obtained from partial radial distribution functions, E_2 (Eq. 7). (a) Ratio of E_2 and E_{sim} vs the number of pseudo species M at $T = 1.0$ (open red symbols) and $T = 0.5$ (filled blue symbols) for different PDIs. (b) Relative error calculation between E_{sim} and E_2 , $(E_2 - E_{sim})/E_{sim}$ plotted as a function of M for different PDIs. For better visualization, we have shifted the y-axis of the 10% PDI plot by 0.1, and 15% PDI plot by 0.2. The horizontal lines signify the corresponding large M values which are 1.0 for (a) and 0.0 for (b). Here particles are interacting via IPL potential and the particle size distribution is given by $P_1(\sigma)$ (constant volume fraction distribution).

ues of T_{cross} at $M = M_0$ and the T_{onset} are given in Table II. Thus we show that the minimum number of pseudo species required to describe the potential energy of the system can also describe the two body excess entropy of the system. Note that although with M_0 pseudo species we can get a reasonable value of S_2 , this quantity is not the total excess entropy of the system. The residual multi-particle entropy (RMPE) defined as the difference between the total excess entropy and the pair excess entropy, $S_{ex} - S_2$ although has a small value when compared to S_2 , plays an important role in describing the thermodynamics of the system. For example, it has been observed that if we ignore RMPE then the correlation between dynamics and thermodynamics expressed via the well known Adam-Gibbs relation does not hold¹². It has also been observed that in the supercooled liquid regime RMPE provides

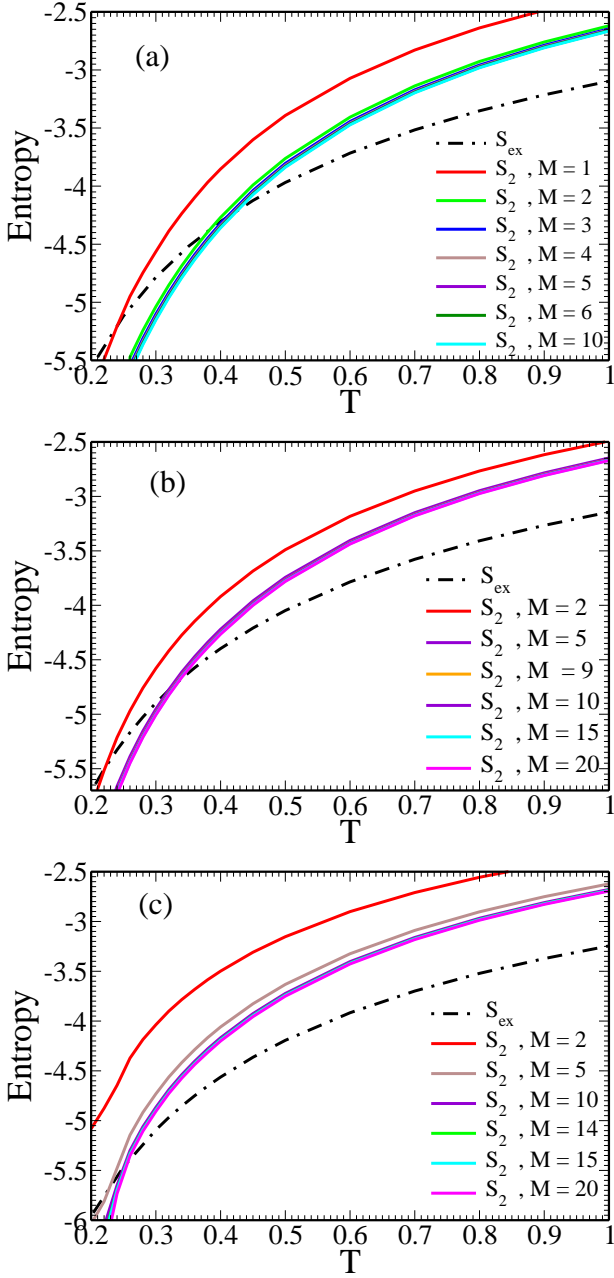


FIG. 6: Excess entropy, S_{ex} , and pair excess entropy S_2 . The latter is calculated at different values of M (Eq.12). Dashed dot line represents S_{ex} and solid lines represent S_2 . (a) PDI 5% (b) PDI 10% (c) PDI 15%. Here particles are interacting via IPL potential and the particle size distribution is given by $P_1(\sigma)$ (constant volume fraction distribution).

us a measure of the activated dynamics of the system^{12,17}. Thus although the pseudo species description provides us a reasonable estimation of S_2 , care should be taken while using this quantity in describing the full thermodynamics of the system.

The details of the M_0 values for the different systems are given in Table II. We also tabulate a quantity $\Delta\sigma_0 = \frac{\Delta\sigma}{M_0}$. We

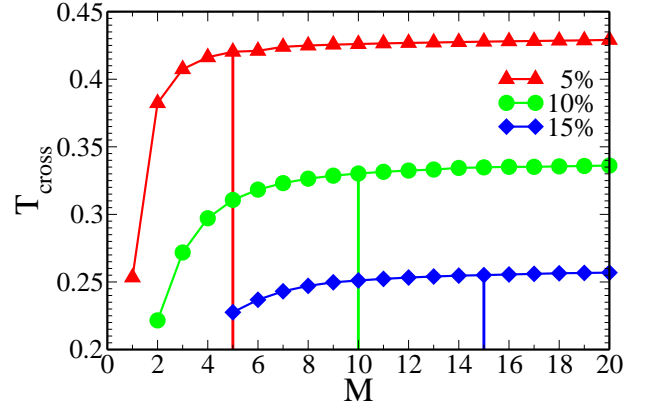


FIG. 7: T_{cross} vs M plot for different PDIs. Initially, T_{cross} increases with M but after certain value of M , it saturates. For larger PDI the saturation takes place at a higher M value. The vertical lines give the value of M_0 obtained from energy criteria. Here particles are interacting via IPL potential and the particle size distribution is given by $P_1(\sigma)$ (constant volume fraction distribution).

find that although M_0 is dependent on the PDI this quantity $\Delta\sigma_0$ is not. Note that when $M = M_0$, the maximum error in assigning a diameter to a particle is $\frac{\Delta\sigma_0}{2}$. Thus our study suggests that the thermodynamic properties of the system studied here are not sensitive to a change in diameter by $\frac{\Delta\sigma_0}{2}$ and for a constant volume fraction polydisperse system interacting via IPL potential when $\Delta\sigma \approx 0.036$ we can treat it as a monodisperse system.

Interestingly we find that when we plot the partial rdf for two consecutive pseudo species, $g_{11}(r)$ and $g_{22}(r)$ (here these two species 1 and 2 have the largest and the second largest number of particles, respectively) for different values of M then for $M = M_0$ the peaks of the two rdfs almost overlap (Fig.8). Thus we can say that when the size difference of the two consecutive species are such that there is a large overlap between the radial distribution functions of two consecutive species then they can be treated as a single species.

TABLE II: The values of M_0 and $\Delta\sigma_0$ for different systems. We also provide the values of T_{cross} at $M = M_0$ and for comparison we give the T_{onset} values obtained from fitting the Inherent structure energy to two straight lines.

Distribution	Potential	PDI %	M_0	$\Delta\sigma_0 = \frac{\Delta\sigma}{M_0}$	$T_{cross}(M_0)$	T_{onset}
$P_1(\sigma)$	IPL	5%	5	0.036	0.42	0.43
		10%	10	0.036	0.33	0.36
		15%	15	0.036	0.26	0.31
$P_2(\sigma)$	IPL	5%	7	0.043	0.43	0.46
		10%	14	0.043	0.35	0.34
		15%	21	0.043	0.28	0.30
$P_1(\sigma)$	WCA	15%	20	0.027	0.58	0.7
	LJ	15%	12	0.045	0.67	0.81

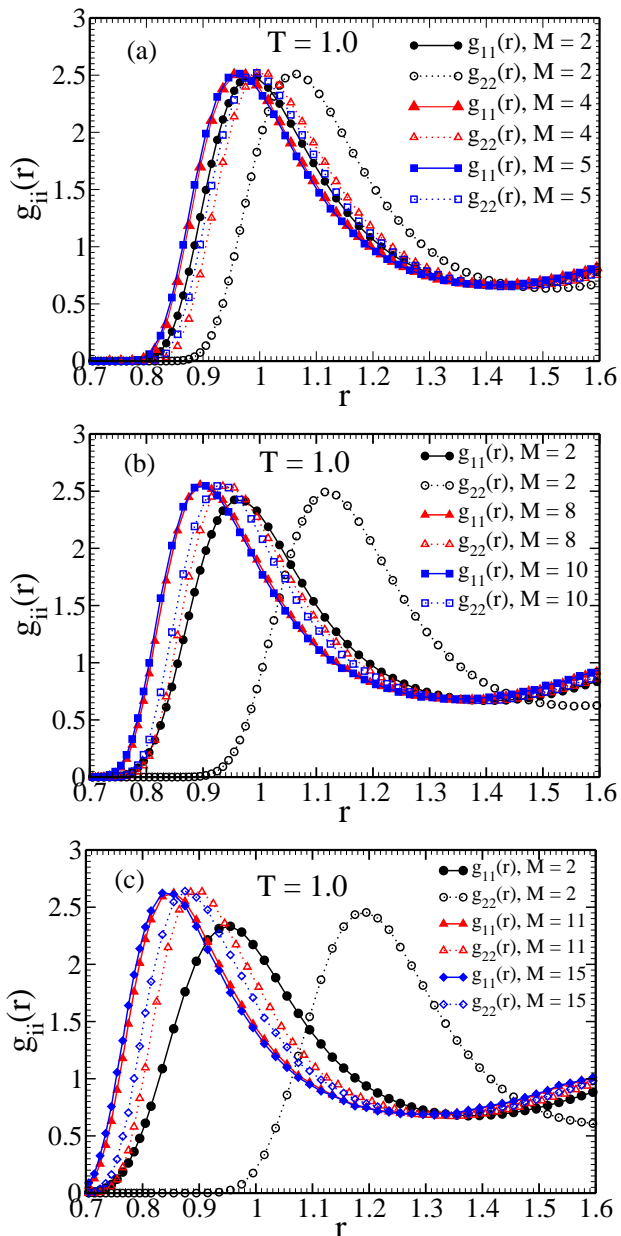


FIG. 8: The partial radial distribution function for the first two species for different values of M . (a) PDI 5% (b) PDI 10% (c) PDI 15%. For $M = M_0$ the rdf peak of the two consecutive species almost overlap. Here particles are interacting via IPL potential and the particle size distribution is given by $P_1(\sigma)$ (constant volume fraction distribution).

C. Effect of the type of distribution on M_0 and $\Delta\sigma_0$

We next study the effect of the type of distribution on M_0 and $\Delta\sigma_0$. In Fig.9 we compare the M dependence of T_{cross} for systems where polydispersity is described in terms of $P_1(\sigma)$ (constant volume fraction) and $P_2(\sigma)$ (Gaussian), for three different PDIs. In the same plot the M_0 values as obtained from the potential energy are also marked.

At the same PDI, the nature of saturation of T_{cross} and also the value of M_0 are different for the two different distributions. Compared to the constant volume fraction distribution, the values of M_0 are higher for the Gaussian distribution. The reason behind this can be understood by comparing Fig.1 and Fig.2 (also see Table I). For the same PDI, the Gaussian distribution is wider compared to the constant volume fraction distribution. A closer observation tells us that the saturation of T_{cross} is better for the CVF distribution when compared to the Gaussian distribution. Note that for the Gaussian distribution M_0 is higher (more number of species), and by nature towards the tail of the distribution the number of particles is less so the partial rdf for the largest and the smallest species are poorly averaged. We have seen that with an increase in system size the saturation improves (not shown here).

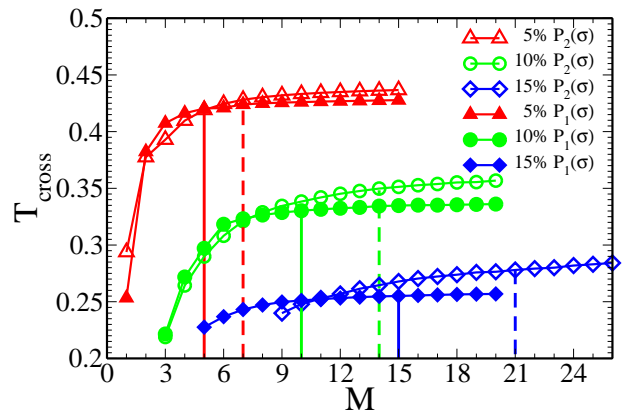


FIG. 9: The effect of the type of distribution on M_0 . T_{cross} vs M plot for different PDIs for systems where particles are interacting via IPL potential and the particle size distribution are given by $P_1(\sigma)$ (constant volume fraction distribution) and $P_2(\sigma)$ (Gaussian distribution). The vertical lines give the value of M_0 obtained from energy criteria (solid lines for P_1 and dashed lines for P_2 distribution). At the same value of PDI for the Gaussian distribution the M_0 is higher and T_{cross} saturates at a higher M value.

We find that when compared to CVF distribution, the $\Delta\sigma_0$ is marginally higher for the systems with Gaussian distribution (see Table II). Note that we divide a continuous poly-disperse system into M species in a way that the difference in diameter of two consecutive species is always separated by $\frac{\Delta\sigma}{M}$. This implies that the percentage error in calculating the size of the smaller particles are higher than that of the larger particles. Also, note that in constant volume fraction distribution the smallest particles are the largest in number thus by construction the error is maximum for the dominant species. On the other hand for the Gaussian distribution, the place where the percentage error is maximum the population of particles are the minimum. Thus compared to the Gaussian distribution for continuous volume fraction we need to go to marginally smaller values of $\Delta\sigma_0$. A way to increase $\Delta\sigma_0$ (decrease M_0) in CVF distribution can be to have a size dependent bin width such that the percentage error in describing the size of a smaller particle is the same as that of a larger particle.

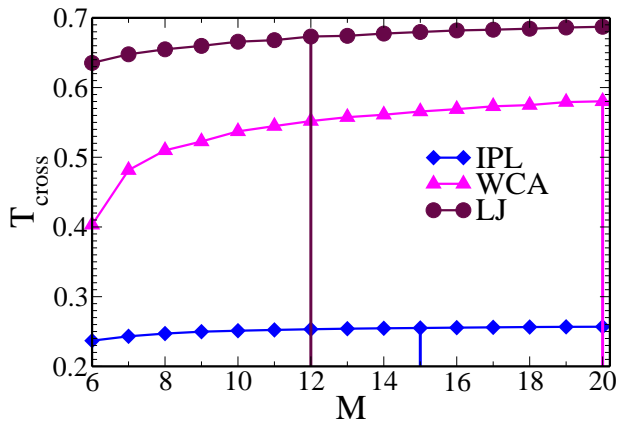


FIG. 10: Role of interaction potential on M_0 . T_{cross} vs M plot for 15% PDIs for systems where particles are interacting via IPL, WCA and LJ potential and the particle size distribution are given by $P_1(\sigma)$ (constant volume fraction distribution). The vertical lines give the value of M_0 obtained from energy criteria. The value of M_0 is higher for WCA potential and the T_{cross} also saturates at higher value of M .

D. Effect of interaction potential on M_0

Next, we study the role of interaction potential on the value of M_0 (also $\Delta\sigma_0$) and the saturation of T_{cross} . For this we study $P_1(\sigma)$ system, with PDI=15% and vary the interaction potential between the particles (IPL, WCA, and LJ). The parameter values are given in Table II. When we compare the IPL, WCA and LJ systems we find that M_0 value is higher for the WCA system and also the T_{cross} of the WCA system appears to saturate at a higher M value (see Fig.10). This suggests that $\Delta\sigma_0$ for the WCA potential is smaller than the LJ and the IPL systems (see Table.II).

To understand the origin of this lower tolerance of the WCA system in Fig.11 we plot for the WCA system the partial rdfs of the first two species for different values of M and find that compared to the IPL system we need to go to higher values of M to observe a good overlap between the two rdfs. Similar to that found for the IPL system, at $M = M_0$ the rdf peaks almost overlap. Note that compared to the WCA potential the IPL potential is softer and has a longer range. Thus compared to the WCA system the IPL system has a flatter rdf and a larger overlap of the rdfs of two consecutive species. This definitely explains why compared to the IPL system the M_0 is higher for the WCA system.

In Fig.12 we compare the rdf values for the first two species of the IPL, WCA and LJ systems, for $M = 15$. Note that for the IPL and the LJ systems $M_0 \leq 15$ and for the WCA system $M_0 > 15$. However, compared to the WCA and IPL systems, the partial rdfs for the LJ system are more sharply peaked. This does not explain why the M_0 for the LJ system is smaller than the WCA system. Note that the structure along with the interaction potential describes both the potential energy and also the two body entropy. In S_2 the leading term is $-g(r) \ln g(r) \simeq g(r)W(r)$ where $W(r) = -\ln g(r)$ can be considered as the effective potential of the system. Thus along with the rdf the interaction potential also plays a role in determining these thermodynamic quantities. The range

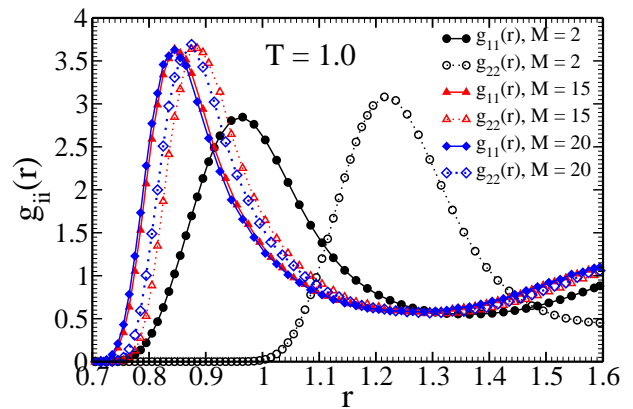


FIG. 11: The partial radial distribution function for the first two species for different values of M . The particles are interacting via WCA potential and the polydispersity of the system is described by $P_1(\sigma)$ with 15% PDI.

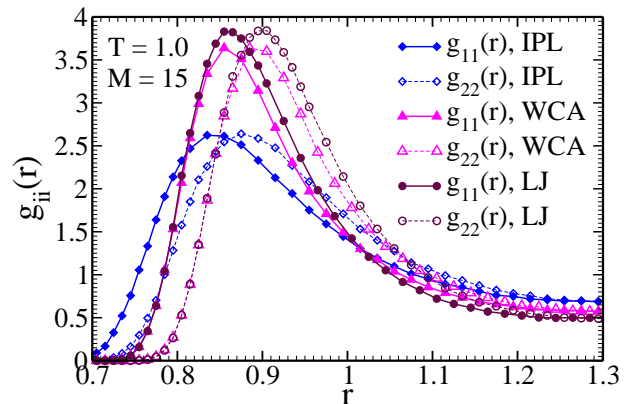


FIG. 12: The partial radial distribution functions for the first two species for IPL, WCL and LJ potentials for $M = 15$. The size distribution of the particles is given by $P_1(\sigma)$ with 15% polydispersity.

of the LJ potential is much larger compared to the IPL and WCA potentials. Moreover, the attractive part of the potential which provides a dominant contribution also varies much more smoothly compared to the WCA and IPL potentials. It appears that this slow variation of the potential increases the tolerance of thermodynamic quantities w.r.t the particle size which leads to a smaller M_0 value.

We will like to mention that in this work while working with the LJ system we only vary the size of the particles while keeping the interaction energy constant. This choice is quite similar to that used in earlier studies of model polydisperse systems^{9,43,44}. However, this choice of system is not consistent with the van der Waals attraction dependence on particle volume. Thus the system can have some unusual structures like that of clustering of smaller particles observed earlier⁴⁴

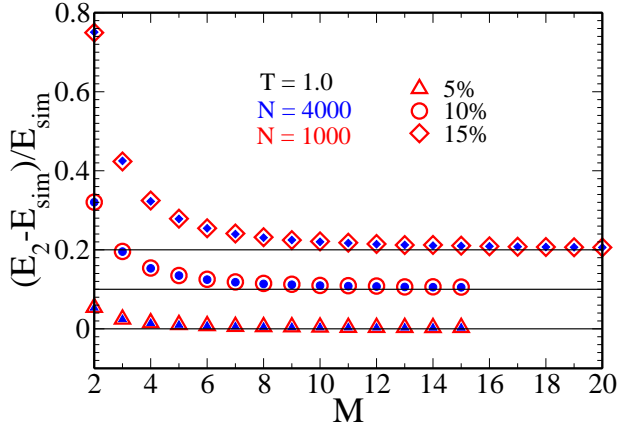


FIG. 13: System size dependence of relative error calculation between E_{sim} and E_2 . $(E_2 - E_{sim})/E_{sim}$ plotted as a function of M for different PDIs for $N = 1000$ (red open symbols) and $N = 4000$ (blue filled symbols). For better visualization, we have shifted the y-axis of the 10% PDI plot by 0.1 and 15% PDI plot by 0.2. The horizontal lines signify the corresponding zero values.

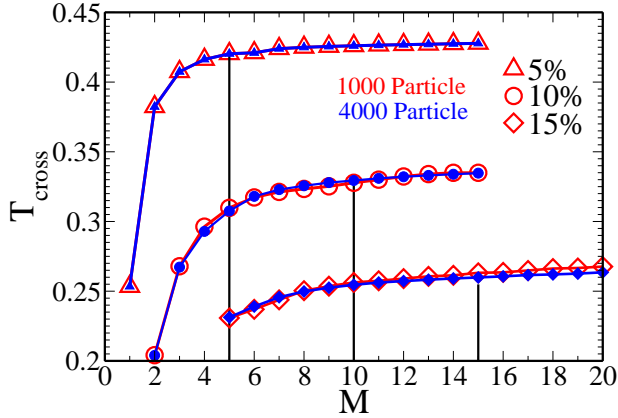


FIG. 14: The system size dependence of M_0 . T_{cross} vs M plot for different PDIs for systems where particles are interacting via IPL potential and the particle size distribution are given by $P_1(\sigma)$. The open red symbols are for $N=1000$ and the filled blue symbols are for $N=4000$. The vertical lines give the value of M_0 obtained from energy criteria. M_0 from energy is independent of system size and for systems with higher PDI the T_{cross} saturates better for higher system size.

E. System size dependence

Note that for finite number of particles (N) in the system, we can still describe the $N \times N$ partial structure factors. However in the thermodynamic limit when $N \rightarrow \infty$ this becomes ill-defined. Thus for larger systems describing the system in terms of pseudo species becomes even more important. In this section, we study the system size dependence of M_0 . For this study, we take the system where particle size distribution

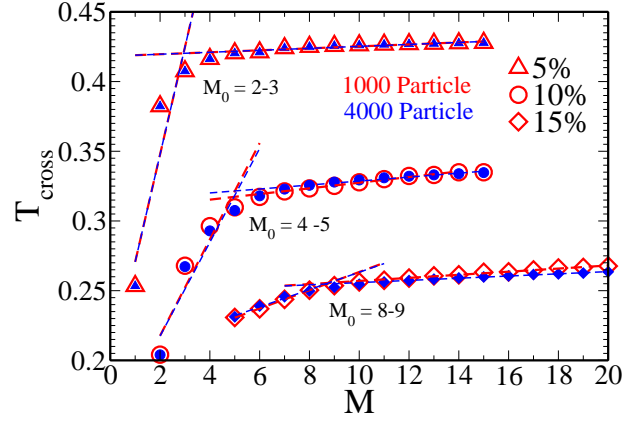


FIG. 15: Alternate definition of M_0 . T_{cross} vs M has two different regimes, low M shows growth and high M shows a near saturation. The two different regimes are fitted to two straight lines and the M value where these lines cross is identified as M_0 . The open red symbols are for $N=1000$ and the filled blue symbols are for $N=4000$. The M_0 values thus obtained are smaller than that obtained from energy criteria and similar to that obtained by Ozawa and Berthier²⁷

is given by $P_1(\sigma)$ and the particles interact via IPL potential. We study three systems at 5%, 10% and 15% PDI. In Fig.13 we plot the $\frac{(E_2 - E_{sim})}{E_{sim}}$ for systems with 1000 and 4000 particles. We find that the relative error in energy is independent of the system size and so is M_0 . In Fig.14 we plot the T_{cross} values for the two different system sizes. We find that for 5% and 10% PDI they overlap and for 15% PDI the bigger system size predicts a better saturation of T_{cross} . This is because we now have a larger number of particles in each species giving rise to better averaging. Thus we can say that M_0 is independent of system size.

F. Comparison with earlier predictions

Next, we compare our results with that of Ozawa and Berthier (OB)²⁷. The goal of both studies is to find an effective number of pseudo species that can describe a polydisperse system. However, the methodologies are quite different. We work with the partial rdf of the liquid and use them to calculate the excess entropy and total energy near the onset temperature. Ozawa and Berthier used the information of the vibrational entropy and the inherent structure properties and the study was performed below the MCT transition temperature. They divided the system into M species and then swapped particles within a species. After N such swaps, they minimized the system and obtained the mean square displacement (MSD) between the original equilibrium configuration and swapped configuration. The MSD as a function of M initially decreased with increasing M and showed saturation at high values of M . They fitted these two regimes to two different power laws, and the intersection point of the power laws determined the value of M_0 . In their study they have calculated the value of M_0 for an IPL potential system with $P_1(\sigma)$ distribution at 23% PDI. They then extrapolated the value of

M_0 for smaller PDIs. For 10% PDI they predicted a value of $M_0 = 4 - 5$ and for 5% PDI, $M_0 = 2 - 3$. We can do a similar exercise with T_{cross} . In Fig.15 we show that T_{cross} also shows two different regimes. We fit the two different regimes to two straight lines and the point where they cross is, $M_0 = 2 - 3$ for 5% PDI, $M_0 = 4 - 5$ for 10% PDI, and $M_0 = 8 - 9$ for 15% PDI. Interestingly these numbers are surprisingly the same as that extrapolated by Ozawa and Berthier²⁷ although the two methodologies are completely different. However, these values of M_0 are lower than our earlier prediction which was made by looking at the saturation point of T_{cross} . In the OB study if they define the M_0 at the value where their MSD becomes independent of M then they too will have a higher value of M_0 .

We next compare our predictions with an earlier work which involved the study of the dynamics²⁶. As discussed in the Introduction, Weysser *et al* studied the effect of polydispersity on the dynamics²⁶. They studied a system with constant polydispersity where $\Delta\sigma = 0.2$. According to their study, the dynamics can be well explained when the system is divided into 5 pseudo species and thus $\Delta\sigma_0 = 0.04$ falls in a similar range as predicted here and so is M_0 .

At this point, we cannot comment on which will be a better choice of M_0 , the value at which T_{cross} saturates or the value at which two different regimes intersect. When we compare our result with the study using the dynamics²⁶ it appears that the former which leads to higher values of M_0 is a better choice whereas if we compare with OB study then the latter seems to be a better choice. It is possible that the dynamics is more sensitive to change in M_0 . This suggests that further studies are required to narrow down the value of M_0 . One such option will be to see how the configurational entropy for different values of M_0 correlates with the dynamics.

V. CONCLUSION

In this work we attempt to develop a framework to describe the structure of systems with continuous polydispersity. The study involves systems where the polydispersity is described in terms of different distributions (constant volume fraction and Gaussian) and the degree of polydispersity is varied. We also study the effect of the interaction potential.

We exploit the fact that the potential energy and the pair excess entropy can be described in terms of the partial radial distribution functions. First, we describe the system in terms of pseudo species. In the case of potential energy, we obtain the minimum number of pseudo species, M_0 required to match the energy obtained from the partial rdf with that obtained from the simulation. For the entropy part, since the excess entropy and pair excess entropy are never equal, we calculate the temperature where they cross each other. Our earlier study has shown that this T_{cross} is an estimate of the onset temperature of supercooled liquids¹⁵. We show that for a smaller number of species, the T_{cross} varies with M and as a function of species this temperature shows a saturation, suggesting a saturation of the pair excess entropy w.r.t M . This gives us a second estimation of M_0 which we find is similar to that obtained from the potential energy.

Our study reveals that for a given system, it is possible to define a parameter $\Delta\sigma_0$ which gives the limiting width of the size distribution that can be treated as a monodisperse system. This limiting value primarily depends on the interac-

tion potential. The softer the interaction potential the larger is the value of $\Delta\sigma_0$. Depending on the type of distribution this limiting width $\Delta\sigma_0$ translates into different values of PDI.

For a 1% PDI system with constant volume fraction distribution, $\Delta\sigma = 0.036$ and with Gaussian distribution, $\Delta\sigma = 0.06$. When we compare these values with $\Delta\sigma_0$, we can say that polydispersity greater than 1% when treated as an effective monodisperse system will not provide us with the correct structure of the liquid. This implies that when the effective one component structure is used to study the influence of polydispersity on some property, we have to be careful in decoupling the effect of this artificial softening of the structure from the actual effect of the polydispersity. Note that M_0 and $\Delta\sigma_0$ are independent of the system size. This makes this pseudo neighbour description of a system more useful for larger systems.

Dedication

This article is dedicated to the memory of Prof. Charusita Chakravarty a mentor and a friend. She not only made a huge contribution in Physical Chemistry, but also was passionate about the upliftment of women scientists. Had she been around she would have definitely felt very happy about this special issue and contributed to it. Her absence has created a void in the field.

Acknowledgment

S. M. B thanks C. Chakravarty, C. Dasgupta, S. Sastry, and B. Bagchi for discussion. P. P. and U. K. N thanks CSIR, for the research fellowships. M. K. N thanks CSIR for funding, S. M. B. thanks SERB for funding.

Availability of Data

The data that support the findings of this study are available from the corresponding author upon reasonable request.

VI. REFERENCES

- ¹X. Xu, G. Friedman, K. D. Humfeld, S. A. Majetich, and S. A. Asher, *Am. Chem. Soc.* **14**, 1249 (2001).
- ²V. K. L. Mer, *Am. Chem. Soc.* **44**, 1270 (1952).
- ³D. A. Kofke and P. G. Bolhuis, *Phys. Rev. E* **59**, 618 (1999).
- ⁴D. J. Lacks and J. R. Wienhoff, *J. Chem. Phys.* **111**, 398 (1999).
- ⁵S. R. Williams, I. K. Snook, and W. van Meegen, *Phys. Rev. E* **64**, 021506 (2001).
- ⁶P. Chaudhuri, S. Karmakar, C. Dasgupta, H. R. Krishnamurthy, and A. K. Sood, *Phys. Rev. Lett.* **95**, 248301 (2005).
- ⁷S. Sarkar, R. Biswas, M. Santra, and B. Bagchi, *Phys. Rev. E* **88**, 022104 (2013).
- ⁸A. Ninarello, L. Berthier, and D. Coslovich, *Phys. Rev. X* **7**, 021039 (2017).
- ⁹S. E. Abraham, S. M. Bhattacharyya, and B. Bagchi, *Phys. Rev. Lett.* **100**, 167801 (2008).
- ¹⁰S. Auer and D. Frenkel, *Nature* **413**, 711 (2001).
- ¹¹A. Banerjee, S. Sengupta, S. Sastry, and S. M. Bhattacharyya, *Phys. Rev. Lett.* **113**, 225701 (2014).
- ¹²M. K. Nandi, A. Banerjee, S. Sengupta, S. Sastry, and S. M. Bhattacharyya, *J. Chem. Phys.* **143**, 174504 (2015).
- ¹³A. Banerjee, M. K. Nandi, S. Sastry, and S. M. Bhattacharyya, *J. Chem. Phys.* **145**, 034502 (2016).
- ¹⁴A. Banerjee, M. K. Nandi, and S. M. Bhattacharyya, *J. Chem. Sci.* **129**, 793 (2017).
- ¹⁵A. Banerjee, M. K. Nandi, S. Sastry, and S. Maitra Bhattacharyya, *J. Chem. Phys.* **147**, 024504 (2017).

- ¹⁶M. K. Nandi, A. Banerjee, C. Dasgupta, and S. M. Bhattacharyya, *Phys. Rev. Lett.* **119**, 265502 (2017).
- ¹⁷M. K. Nandi and S. Maitra Bhattacharyya, *J. Chem. Phys.* **148**, 034504 (2018).
- ¹⁸I. Saha, M. K. Nandi, C. Dasgupta, and S. M. Bhattacharyya, *J. Stat. Mech.: Theory Exp* **2019**, 084008 (2019).
- ¹⁹M. K. Nandi and S. Maitra Bhattacharyya, arXiv:2011.02299v1 (2020).
- ²⁰D. Frydel and S. A. Rice, *Phys. Rev. E* **71**, 041403 (2005).
- ²¹C. P. Royall, A. A. Louis, and H. Tanaka, *J. Chem. Phys.* **127**, 044507 (2007).
- ²²P. Salgi and R. Rajagopalan, *Adv. Colloid Interface Sci.* **43**, 169 (1993).
- ²³T. O. Pangburn and M. A. Bevan, *J. Chem. Phys.* **123**, 174904 (2005).
- ²⁴T. O. Pangburn and M. A. Bevan, *J. Chem. Phys.* **124**, 054712 (2006).
- ²⁵M. J. Pond, J. R. Errington, and T. M. Truskett, *J. Chem. Phys.* **135**, 124513 (2011).
- ²⁶F. Weysser, A. M. Puertas, M. Fuchs, and T. Voigtmann, *Phys. Rev. E* **82**, 011504 (2010).
- ²⁷M. Ozawa and L. Berthier, *J. Chem. Phys.* **146**, 014502 (2017).
- ²⁸D. L. Majure *et al.*, *IEEE*, 201 (2008).
- ²⁹R. Gutiérrez, S. Karmakar, Y. G. Pollack, and I. Procaccia, *EPL* **111**, 56009 (2015).
- ³⁰J. E. Jones and S. Chapman, *R. Soc.* **106**, 463 (1924).
- ³¹J. D. Weeks, D. Chandler, and H. C. Andersen, *J. Chem. Phys.* **54**, 5237 (1971).
- ³²J. P. Hansen and I. R. McDonald, 2nd ed., Academic, London (1986).
- ³³M. Singh, M. Agarwal, D. Dhabal, and C. Chakravarty, *J. Chem. Phys.* **137**, 024508 (2012).
- ³⁴J. G. Kirkwood and E. M. Boggs, *J. Chem. Phys.* **10**, 394 (1942).
- ³⁵T. Goel, C. N. Patra, T. Mukherjee, and C. Chakravarty, *J. Chem. Phys.* **129**, 164904 (2008).
- ³⁶S. Sastry, P. G. Debenedetti, and F. H. Stillinger, *Nature* **393**, 554 (1998).
- ³⁷S. Sengupta, F. Vasconcelos, F. Affouard, and S. Sastry, *J. Chem. Phys.* **135**, 194503 (2011).
- ³⁸P. Giaquinta and G. Giunta, *Physica A: Stat. Mech. and its Appl.* **187**, 145 (1992).
- ³⁹G. P. V. Prestipino Santi, *J. stat. Phys.* **96**, 135 (1999).
- ⁴⁰F. Saija, S. Prestipino, and P. V. Giaquinta, *J. Chem. Phys.* **113**, 2806 (2000).
- ⁴¹F. Saija, S. Prestipino, and P. V. Giaquinta, *J. Chem. Phys.* **124**, 244504 (2006).
- ⁴²J. Mittal, J. R. Errington, and T. M. Truskett, *J. Chem. Phys.* **125**, 076102 (2006).
- ⁴³N. Kiriushcheva and P. H. Poole, *Phys. Rev. E* **65**, 011402 (2001).
- ⁴⁴T. S. Ingebrigtsen and H. Tanaka, *J. Phys. Chem. B* **119**, 11052 (2015).